

Energy and Enstrophy Transfer in Decaying Two-Dimensional Turbulence

M. K. Rivera,^{1,2} W. B. Daniel,^{1,2} S. Y. Chen,^{2,3} and R. E. Ecke^{1,2}

¹*Condensed Matter & Thermal Physics Group, Los Alamos National Laboratory, Los Alamos, New Mexico 87545*

²*Center for Nonlinear Studies, Los Alamos National Laboratory, Los Alamos, New Mexico 87545*

³*Department of Mechanical Engineering, The Johns Hopkins University, Baltimore, Maryland 21218*

(Received 22 October 2002; published 13 March 2003)

We present experimental data on the direct enstrophy cascade in decaying two-dimensional turbulence. Velocity and vorticity fields are obtained using particle tracking velocimetry. From those fields we directly compute the enstrophy and energy flux by using a filtering technique inspired by large-eddy simulations. This allows considerable insight into the physical processes of turbulence when compared with structure-function or spectral analysis. The direct cascade of enstrophy is weakly forward, with almost as much backscatter as down-scale enstrophy transfer, whereas the inverse energy cascade is strongly upscale with a modest amount of backscatter.

DOI: 10.1103/PhysRevLett.90.104502

PACS numbers: 47.27.-i, 47.32.-y

Conclusions about how kinetic energy or enstrophy are transported from one length scale to another in a turbulent fluid are often obtained through the comparison of measured velocity or vorticity structure functions with predictions obtained by theoretical models [1,2]. There is considerable ambiguity in this approach: The scaling behavior of a given structure function is not necessarily connected with the scale-to-scale transport property assumed in the model. This approach is also limited to exploring average scale-to-scale transport throughout the bulk of the fluid, rather than the local transport in a given region. Considering the importance of scale-to-scale transport in turbulence phenomenology, more informative measurement techniques are necessary to establish transport behavior in turbulent fluids.

An alternative to the structure-function approach is a filter-space technique (FST) that prescribes a general method for measuring the scale-to-scale transport of a given quantity. In this method, the flow is separated into large-scale and small-scale components, as is done in large-eddy direct numerical simulations (DNS) [2,3], from which the interaction between the two components can be determined. A similar approach was first proposed by Kraichnan [4], and has recently been used to analyze numerical simulations of 2D and 3D turbulence [5,6].

Here, the scale-to-scale energy and enstrophy transport in decaying 2D turbulence in a soap-film channel is investigated using FST. For length scales around and below the energy injection scale, l_{inj} , the average scale-to-scale energy flux in decaying 2D turbulence is upscale, that is, energy is transported from small to large scales, and the average enstrophy flux is in the opposite direction, i.e., down scale. Neither of the quantities, however, obtains a constant flux for length scales smaller than l_{inj} , thus neither energy nor enstrophy is being transported inertially through this range of scales. For length scales larger than l_{inj} , however, the energy flux seems to asymptote to a constant value, indicative of inertial transport.

Probability distribution functions (PDFs) of energy and enstrophy flux reveal that the enstrophy flux for scales around l_{inj} is less efficient than energy transfer: There is a higher probability of finding enstrophy being transported against the mean direction (i.e., upscale) than for energy.

The experimental measurements were carried out in a flowing soap-film channel, a quasi-2D system for which decaying turbulence of low to moderate Reynolds number ($10^2 \leq Re \leq 10^4$) can be easily generated. The channel was 5 cm wide and was inclined at an angle of 60° with respect to vertical. The mean flow was 150 cm/s and the film thickness was 15 μm . A more detailed description of the channel can be found in [7,8]. Using the empirical relationships measured in [9], the film's kinematic viscosity was $\nu \approx 0.03 \text{ cm}^2/\text{s}$. The turbulence generating grid used rods of 0.12 cm diameter with 0.22 cm spacing between the rods. Thus, the blocking fraction is around 0.3, which may seem high when compared with 3D turbulence experiments, but is the standard configuration for obtaining significant turbulence in 2D soap-film flows [7,10,11]. The resultant Reynolds number, $Re = ul/\nu$, was 1100 based on the mean-flow velocity and the injection scale of $l_{inj} = 0.22 \text{ cm}$. The turbulent velocity $\mathbf{u}(\mathbf{x})$ and vorticity $\omega(\mathbf{x})$ fields created by the grid were obtained by tracking 3–5 μm hollow glass spheres (density approximately 1.2 g/cc) within a $1 \times 1 \text{ cm}^2$ region located 1.5 cm downstream of the grid (20–30 eddy rotation times) [12,13]. The particles were illuminated with a double pulsed Nd:YAG laser and their images captured by a 1024×1024 pixel camera. More than 10^4 particles were individually tracked for each image pair and their velocities and local shears were interpolated to a discrete 65×65 grid. Five-hundred velocity and vorticity fields were obtained in this way. A typical vorticity field is shown in Fig. 1(a).

The current phenomenological model of 2D turbulence is based largely upon the work of Kraichnan [14,15] and Batchelor [16]. In 2D turbulent systems, there are two

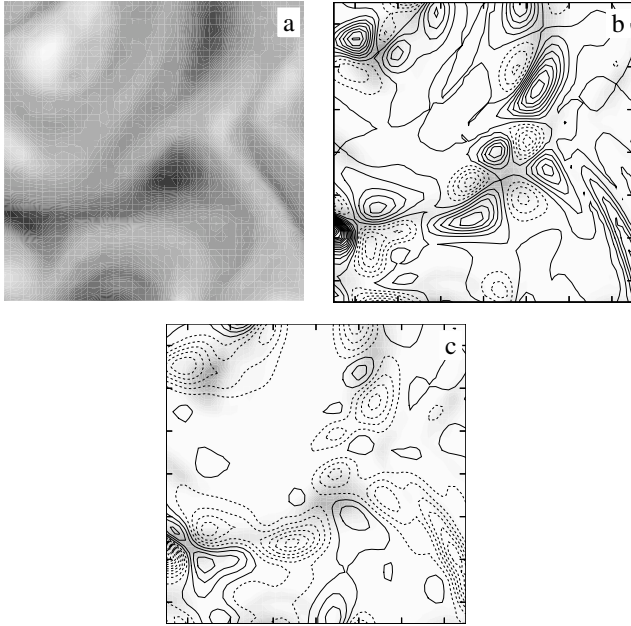


FIG. 1. (a) Vorticity field (white positive, black negative), (b) enstrophy flux isocontours, $Z^{(l)}$, and (c) energy flux isocontours, $Q^{(l)}$, for $l \approx 0.13$ cm. Dashed isocontours represent negative values of energy or enstrophy flux. The isocontours are superimposed upon the enstrophy field (darker color represents increasing values of enstrophy). The hatch marks represent 1 mm increments.

ranges bracketing the injection length scale, l_{inj} , through which energy (mean-square velocity, $|\mathbf{u}|^2/2$) or enstrophy (mean-square vorticity, $\omega^2/2$) can be transferred inertially. The direct cascade range exists for length scales $l_\nu < l < l_{inj}$ and transports enstrophy from the injection scale to the viscous scale l_ν . In the inverse cascade range, energy is transported from l_{inj} to scales larger than the injection scale until some boundary scale, set by either the physical system size or an external dissipation mechanism, is encountered. Inertial transfer defines the condition where enstrophy or energy is transferred between scales without loss. An inertial range is, therefore, a range of length scale characterized by a constant energy or enstrophy flux.

Given the above picture and using various assumptions, one can show that in an inertial direct cascade range the second-order structure functions of longitudinal velocity difference, $S_2(r) \equiv \langle ([\mathbf{u}(\mathbf{x} + \mathbf{r}) - \mathbf{u}(\mathbf{x})] \cdot \hat{\mathbf{r}})^2 \rangle$, and the second-order structure function of vorticity difference, $\delta\Omega_2(r) \equiv \langle (\omega(\mathbf{x} + \mathbf{r}) - \omega(\mathbf{x}))^2 \rangle$, should scale as r^2 and r^0 , respectively (with logarithmic corrections to the latter) [17]. Here $\langle \cdot \rangle$ denotes an ensemble average and $r \equiv l/l_{inj}$. If an inertial inverse energy cascade range exists, then $S_2(r)$ should scale as $r^{2/3}$ and $\delta\Omega_2(r)$ as $r^{-1/3}$.

Measurements of these structure functions are shown in Fig. 2. The functions, although not an exact match to the theoretical predictions, are in approximate agreement with theory in the direct cascade range, i.e., for $l < l_{inj}$.

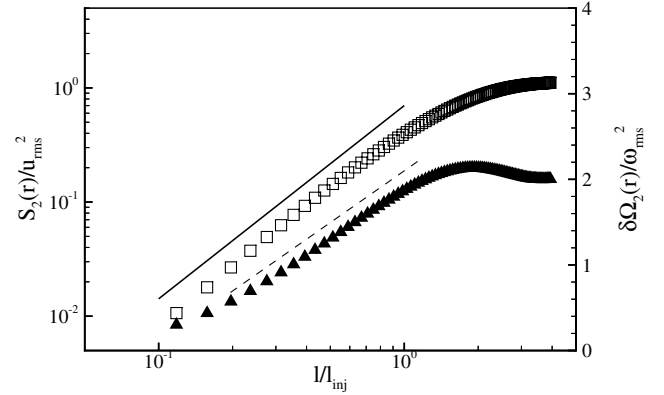


FIG. 2. The second moment of longitudinal velocity difference, $S_2(r)$ (\square), and the second moment of vorticity difference, $\delta\Omega_2(r)$ (\blacktriangle), as a function of $r \equiv l/l_{inj}$. The solid line represents a power law fit of $S_2(r)$ yielding an exponent of 1.7. The dashed line indicates a logarithmic dependence of $\delta\Omega_2(r)$.

Moreover, there seems to be no scaling behavior at length scales larger than the injection scale. Plots such as those in Fig. 2 are typical of 2D decaying turbulence systems [7,10,11] and are interpreted as evidence for an inertial direct enstrophy cascade. Similarly, the absence of structure-function scaling for $l > l_{inj}$ implies that there is no inertial energy cascade. The problem is that these conclusions are indirect and nothing further can be obtained from the structure-function approach. In contrast, FST provides a direct measure of inertial transport. Its application to the experimental data will demonstrate that the indirect conclusions drawn from structure-function analysis are incorrect.

The objective of FST is to transform the measured fields $\mathbf{u}(\mathbf{x})$ and $\omega(\mathbf{x})$ into spatially local scale-to-scale energy and enstrophy transport information [5]. This will be done below for enstrophy flux; the extension of the technique to the case of energy flux is straightforward. Start by defining a filter function, $G^{(l)}$, with a typical length scale, l . Although the exact nature of $G^{(l)}$ is not important for this technique, for concreteness take $G^{(l)}$ to be a Gaussian of k space half-width $\tau \equiv 2\pi/l$. Applying the filter function $G^{(l)}$ to an arbitrary field $f(\mathbf{x})$ yields the large-scale field, $f_l(\mathbf{x})$, i.e., a field with Fourier modes larger than $2\pi/l$ suppressed. Convolving the filter function with Euler's equation for vorticity in a 2D fluid yields

$$\frac{\partial \omega_l}{\partial t} + (u_s)_l \frac{\partial \omega_l}{\partial x_s} = - \frac{\partial}{\partial x_s} \sigma_s^{(l)}, \quad (1)$$

where $\sigma_s^{(l)} \equiv (\omega u_s)_l - (u_s)_l \omega_l$. The Einstein summation rule is used here over the subscript s (not over l). The large-scale field advects in the same manner as the full field, that is to say the left side is simply the Euler equation for the large-scale field. In addition, there exist a coupling term on the right-hand side that accounts for

the motion of large-scale vorticity by small-scale fluctuations.

The evolution equation for the large-scale enstrophy, $\Omega^{(l)} \equiv \frac{1}{2} \omega_l^2$, within which the coupling term, taking the form $\omega_l \partial_s \sigma_s^{(l)}$, is obtained by multiplying Eq. (1) by the large-scale vorticity, ω_l . The coupling term can affect the large-scale enstrophy at a given point in two ways: by spatially redistributing large-scale enstrophy or by moving enstrophy contained in wave numbers above $2\pi/l$ to wave numbers below $2\pi/l$. The latter of these two mechanisms is the scale-to-scale enstrophy transport term. To separate it out, utilize the Leibniz rule on the right-hand side to obtain

$$\frac{\partial}{\partial t} \Omega^{(l)} + \frac{\partial}{\partial x_s} (u_s)_l \Omega^{(l)} = - \frac{\partial}{\partial x_s} (\sigma_s^{(l)} \omega_l) + \sigma_s^{(l)} \frac{\partial \omega_l}{\partial x_s}. \quad (2)$$

Under homogenous conditions, the ensemble average of the first term on the right-hand side disappears. This term is associated with spatial redistribution of enstrophy. The second term represents scale-to-scale transport of enstrophy. We define $Z^{(l)} \equiv -\sigma_s^{(l)} [(\partial \omega_l) / (\partial x_s)]$ as the scale-to-scale enstrophy transport through a length scale l . The negative sign is used so that positive $Z^{(l)}$ represents down-scale transfer of enstrophy and negative represents up-scale transfer. A similar set of equations can be derived for energy transport starting from the 2D Euler equations for velocity. In that case, the scale-to-scale transport of energy is written $Q^{(l)} \equiv -\xi_{rs}^{(l)} \{[\partial (u_r)_l] / (\partial x_s)\}$ with $\xi_{rs}^{(l)} \equiv (u_r u_s)_l - (u_s)_l (u_r)_l$ and the same sign convention as for $Z^{(l)}$.

A determination of $Z^{(l)}$ and $Q^{(l)}$ from the soap-film data yields typical flux isocontours shown in Figs. 1(b) and 1(c). The isocontours have been superimposed onto the enstrophy field, $\Omega \equiv \omega^2/2$. Continuous regions with large values of enstrophy (dark regions) correspond to vortices. The extrema of the scale-to-scale energy and enstrophy flux isocontours are both grouped about the edges of vortices, whereas regions removed from strong vortices have comparatively weak flux fields. There is considerable cancellation so that strong conclusions regarding correlations of flow structures with mean transfer cannot be made at this time. Nevertheless, these strong vortices contribute heavily to the wings of the transfer PDFs and are important features of the flow.

To obtain a quantitative measure of the average energy and enstrophy transfer, the PDFs of 500 statistically independent $Z^{(l)}$ and $Q^{(l)}$ fields were evaluated for a range of length scales l . The PDFs, shown in Fig. 3, have been normalized by their respective rms fluctuations but the mean has not been removed. The behavior of the two distributions is markedly different. Although both are asymmetric, the enstrophy flux distribution is positively skewed whereas the energy flux is negatively skewed. The mean values of the PDFs are plotted as a function of scale in Fig. 4, where one sees that the average energy flux is

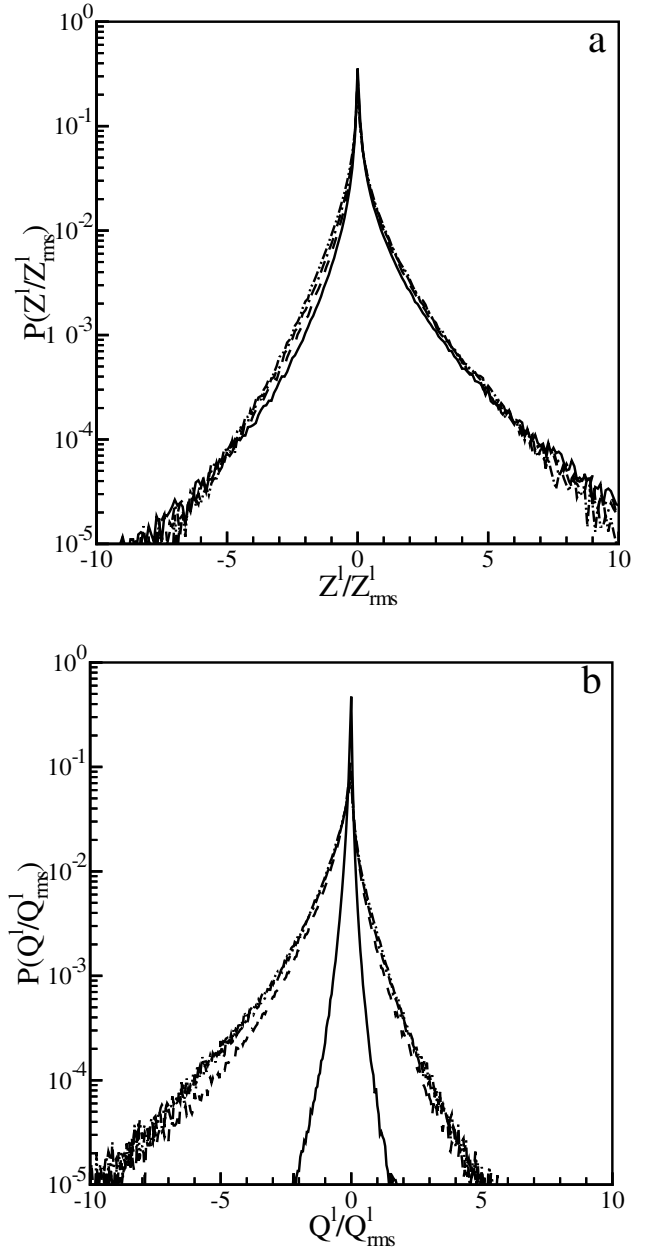


FIG. 3. Normalized probability distribution functions for (a) the scale-to-scale enstrophy flux $Z^{(l)}$ and (b) the scale-to-scale energy flux $Q^{(l)}$ evaluated at length scales $l = 0.06$ cm (solid line), $l = 0.1$ cm (dashed line), $l = 0.15$ cm (dash-dotted line), and $l = 0.2$ cm (dash-dot-dotted line).

upscale and the average enstrophy flux is predominantly down scale.

The average enstrophy flux shown in Fig. 4 never becomes constant. Therefore in the soap-film channel an inertial enstrophy flux range is not achieved, in direct contradiction to the conclusions drawn from the structure-function analysis. Rather, the average flux increases slightly below the injection scale, then falls off at scales below half the injection scale. The increase below the injection scale may arise from the injection of enstrophy

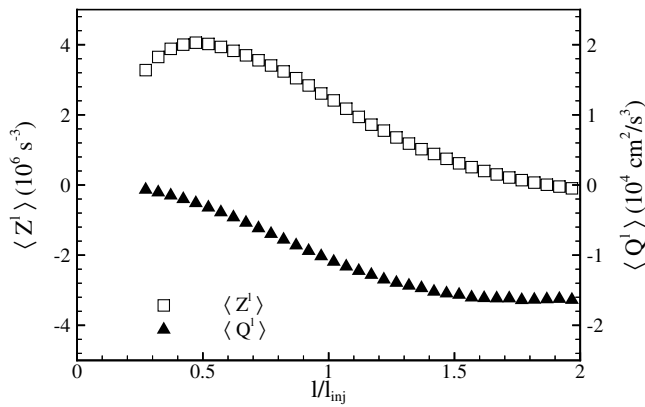


FIG. 4. The average enstrophy (\square) and energy flux (\blacktriangle) as a function of length scale l/l_{inj} .

over a range of length scales around l_{inj} rather than at precisely this scale. The fall off in enstrophy transfer at small scales is due to the frictional effects of air drag acting on the soap-film channel. Results from numerical simulations, to be presented elsewhere, find almost identical behavior in the enstrophy flux when a linear frictional drag is included in the equations of motion.

In contrast to the enstrophy flux, the average energy flux does asymptote at length scales larger than the injection scale. Although more extensive measurements are needed, the flattening of the energy flux at a negative value is indicative of a range of scales through which energy transfer is upscale and inertial. The average energy flux also effectively disappears for length scales smaller than half the injection scale, i.e., at the same length scale where the average enstrophy flux begins to decay. The exact behavior of the curves in Fig. 4 is somewhat dependent on the form of the filter function, $G^{(l)}$. A number of sharper filter functions of the form $e^{-|k|/\tau^m}$ for $m > 2$ were used in the FST analysis without significantly affecting the above conclusions ($m = 2$ is the Gaussian filter).

The PDFs in Fig. 3 can also be used to quantify the amount of backscatter present in the energy or enstrophy flux. Backscatter is defined here as the motion of energy or enstrophy opposite the direction of the mean. In the case of enstrophy, the difference in the probability of down-scale to upscale transfer, $\delta P(Z^{(l)}) \equiv |P(Z^{(l)} > 0) - P(Z^{(l)} < 0)| = 0.1$ for length scales smaller than the injection scale. The same quantity for energy transfer,

$\delta P(Q^{(l)}) = 0.4$ for length scales between the injection scale and half the injection scale. At scales smaller than this, the backscatter of energy quickly disappears. Thus, the mechanism driving upscale energy flux in decaying turbulence is considerably more efficient, i.e., contains less backscatter, than its counterpart driving down-scale enstrophy transfer. The degree of asymmetry found in the enstrophy flux PDF is larger than similar results obtained using 2D numerical simulations [5], where $\delta P[Z^{(l)}] = 0.01$. The simulations, however, were performed at higher effective Reynolds number and were forced rather than decaying. Surprisingly, the magnitude of asymmetry found in the energy flux PDFs is comparable to results obtained in DNS of 3D turbulence [6].

We are grateful to G. Eyink for interesting discussions about FST. This research was supported by the U.S. Department of Energy (W-7405-ENG-36).

-
- [1] U. Frisch, *Turbulence: The Legacy of A. N. Kolmogorov* (Cambridge University Press, Cambridge, England, 1995).
 - [2] M. Lesieur, *Turbulence in Fluids* (Kluwer, Dordrecht, 1987).
 - [3] C. Meneveau and J. Katz, *Annu. Rev. Fluid Mech.* **32**, 1 (2000).
 - [4] R. Kraichnan, *J. Fluid Mech.* **62**, 305 (1974).
 - [5] X. Wang, S. Chen, R. Ecke, and G. Eyink (to be published).
 - [6] S. Cerutti and C. Meneveau, *Phys. Fluids* **10**, 928 (1998).
 - [7] M. Rivera, P. Vorobieff, and R. Ecke, *Phys. Rev. Lett.* **81**, 1417 (1998).
 - [8] P. Vorobieff, M. Rivera, and R. Ecke, *Phys. Fluids* **11**, 2167 (1999).
 - [9] P. Vorobieff and R. Ecke, *Phys. Rev. E* **60**, 2953 (1999).
 - [10] M. Gharib and P. Derango, *Physica (Amsterdam)* **37D**, 406 (1989).
 - [11] H. Kellay, X. Wu, and W. Goldburg, *Phys. Rev. Lett.* **74**, 3975 (1995).
 - [12] M. Ishikawa, Y. Murai, and F. Yamamoto, *Meas. Sci. Technol.* **11**, 677 (2000).
 - [13] K. Ohmi and H. Li, *Exp. Fluids* **11**, 603 (2000).
 - [14] R. Kraichnan, *Phys. Fluids* **10**, 1417 (1967).
 - [15] R. Kraichnan and D. Montgomery, *Rep. Prog. Phys.* **43**, 547 (1980).
 - [16] G. K. Batchelor, *Phys. Fluids (Suppl. II)* **12**, 233 (1969).
 - [17] R. Kraichnan, *J. Fluid Mech.* **47**, 525 (1971).